NASA/TM—2001–211194

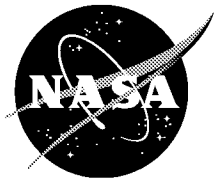

Evaluation of Microcracking in Two Carbon-Fiber/Epoxy-Matrix Composite Cryogenic Tanks

A.J. Hodge
Marshall Space Flight Center, Marshall Space Flight Center, Alabama

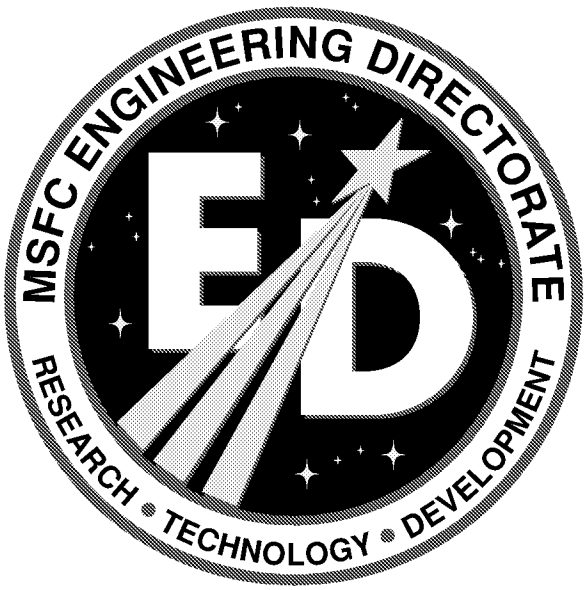

August 2001

The NASA STI Program Office…in Profile

Since its founding, NASA has been dedicated to the advancement of aeronautics and space science. The NASA Scientific and Technical Information (STI) Program Office plays a key part in helping NASA maintain this important role.

The NASA STI Program Office is operated by Langley Research Center, the lead center for NASA's scientific and technical information. The NASA STI Program Office provides access to the NASA STI Database, the largest collection of aeronautical and space science STI in the world. The Program Office is also NASA's institutional mechanism for disseminating the results of its research and development activities. These results are published by NASA in the NASA STI Report Series, which includes the following report types:

- TECHNICAL PUBLICATION. Reports of completed research or a major significant phase of research that present the results of NASA programs and include extensive data or theoretical analysis. Includes compilations of significant scientific and technical data and information deemed to be of continuing reference value. NASA's counterpart of peer-reviewed formal professional papers but has less stringent limitations on manuscript length and extent of graphic presentations.

- TECHNICAL MEMORANDUM. Scientific and technical findings that are preliminary or of specialized interest, e.g., quick release reports, working papers, and bibliographies that contain minimal annotation. Does not contain extensive analysis.

- CONTRACTOR REPORT. Scientific and technical findings by NASA-sponsored contractors and grantees.

- CONFERENCE PUBLICATION. Collected papers from scientific and technical conferences, symposia, seminars, or other meetings sponsored or cosponsored by NASA.

- SPECIAL PUBLICATION. Scientific, technical, or historical information from NASA programs, projects, and mission, often concerned with subjects having substantial public interest.

- TECHNICAL TRANSLATION. English-language translations of foreign scientific and technical material pertinent to NASA's mission.

Specialized services that complement the STI Program Office's diverse offerings include creating custom thesauri, building customized databases, organizing and publishing research results…even providing videos.

For more information about the NASA STI Program Office, see the following:

- Access the NASA STI Program Home Page at ***http://www.sti.nasa.gov***

- E-mail your question via the Internet to help@sti.nasa.gov

- Fax your question to the NASA Access Help Desk at (301) 621–0134

- Telephone the NASA Access Help Desk at (301) 621–0390

- Write to:
  NASA Access Help Desk
  NASA Center for AeroSpace Information
  7121 Standard Drive
  Hanover, MD 21076–1320

NASA/TM—2001–211194

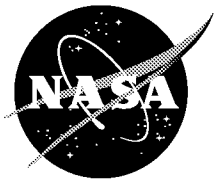

Evaluation of Microcracking in Two Carbon-Fiber/Epoxy-Matrix Composite Cryogenic Tanks

A.J. Hodge
Marshall Space Flight Center, Marshall Space Flight Center, Alabama

National Aeronautics and
Space Administration

Marshall Space Flight Center • MSFC, Alabama 35812

August 2001

Available from:

NASA Center for AeroSpace Information
7121 Standard Drive
Hanover, MD 21076–1320
(301) 621–0390

National Technical Information Service
5285 Port Royal Road
Springfield, VA 22161
(703) 487–4650

TABLE OF CONTENTS

LIST OF FIGURES

LIST OF ACRONYMS AND ABBREVIATIONS

CBAT	Composite Conformal, Cryogenic, Common Bulkhead, Aerogel-Insulated Tank
CLT	Classical Lamination Theory
CTE	coefficient of thermal expansion
LH_2	liquid hydrogen
MSFC	Marshall Space Flight Center

NOMENCLATURE

A	microcrack surface area
b	uncracked layer of laminate
d	transverse, cracked layer of laminate
C	Integration constant
E	modulus
$F(\sigma)$	sum of the mechanically and thermally induced stress
G	critical strain energy release rate
h	half the distance between existing cracks
H	constant
Q	geometry factor
u	displacement in the b layer
v	displacement in the d layer
U	strain energy
W	work
ΔT	change in temperature
σ	stress

TECHNICAL MEMORANDUM

EVALUATION OF MICROCRACKING IN TWO CARBON-FIBER/EPOXY-MATRIX COMPOSITE CRYOGENIC TANKS

1. INTRODUCTION

When a composite laminate is stressed, several damage modes such as matrix microcracking, delamination, and fiber breakage are often observed before final failure. Matrix microcracking is generally the first damage mode observed in a laminated composite. Microcracking generally occurs at load conditions well below final fracture and generally has little effect on the overall strength of the composite laminate. However, microcracking can lead to other damage modes, alter the elastic properties, and increase the laminates' permeability to gases and liquids. Increased permeability is of particular concern when the composite is used as a pressure vessel.

Microcracks typically initiate in plys transversely oriented to the applied load. The transverse load is a result of both mechanical and thermal load. Because of the coefficient of thermal expansion (CTE) mismatch between axially and transversely oriented plys, high residual tensile stresses occur in the transverse direction of a composite ply when the composite laminate is cooled following cure. Further cooling in cryogenic applications exacerbates this condition. Microcracking can occur in some laminates due to thermal effects alone.

The microcracking characteristics of two different composite tanks were evaluated. The microstructure of the X–33 liquid hydrogen (LH_2) tank was examined. Laminates representative of the Marshall Space Flight Center (MSFC) Composite Conformal, Cryogenic, Common Bulkhead, Aerogel-Insulated Tank (CBAT) were also examined. Tensile tests were performed on the laminates to induce microcracking. The tensile tests were performed at ambient and cryogenic temperatures. The microcrack density and applied stress were recorded. A model successfully predicted microcrack density in the X–33 laminate but was less successful with the CBAT laminate.

2. TESTING

2.1 Composite Conformal, Cryogenic, Common Bulkhead, Aerogel-Insulated Tank

The CBAT was constructed of a combination of hand-laid fabric and polar-wound tow. Flat panels representative of the tank acreage were fabricated for microcracking experiments. Tensile specimens were machined from the flat panels. The layup was $(45F/\pm6T/90F_2/\pm6T)_S$ orientation of IM7/977–2 material and the specimens were machined in the *Y* (90 deg) orientation. By loading the laminate in the *Y* orientation, transverse stress was applied to the ±6 plys. Tensile specimens were tested at –320 °F and 72 °F. The specimens were pulled to incrementally higher loads before being cross-sectioned and examined for microcracks.

While immersed in liquid nitrogen, eight specimens were loaded to 4.6, 8.8, 14.4, 18.4, 21.4, 26.5, 46.2, and 60.1 ksi. After testing, the samples were sectioned longitudinally with a water-cooled diamond saw. The cross sections were polished and examined for microcracks at × 50 and × 100 magnification. The microcracks generally spanned the entire width of the test specimen. The microcracks also spanned the thickness of the ±6 ply group. Therefore, no cross sections were performed on the room temperature tests. Only the polished edges of samples were observed. This allowed the same sample to be tested at smaller loading increments and observed between loading cycles until tensile failure.

2.2 X–33 Liquid Hydrogen Tank

The X–33 LH_2 tank lobes were a sandwich construction. A failure occurred after the 42.5 psi LH_2 proof test. The inner skin of one of the lobes separated from the sandwich honeycomb core due to pressure buildup in the honeycomb core. The inner skin was of interest in this study, because microcracking was observed in the inner skin.[1] Tests performed during the X–33 failure investigation determined that mechanical loading at room temperature or thermal cycling without mechanical loading initiate microcracks only in the outer ply of the laminate. The investigation determined that extensive microcracking occurred throughout the inner skin of the tank during the proof test due to a combination of the thermal and mechanical loads. The X–33 LH_2 tank failure investigation concluded microcracking allowed hydrogen infiltration into the sandwich core.[1] The investigation also concluded that studies on microcracking of composite laminates while under load at cryogenic temperatures are needed.[1]

The inner skin of the lobes was 13 plys of IM7/977–2 fiber-placed tow in a $(45/90_3/–45/0_{1.5})_S$ orientation. The 0-deg plys were oriented in the longitudinal direction. Significant cracking was observed in the 45- and 90-deg plys, while lower densities were observed on the 0-deg plys. Cracks in the –45-deg plys were a rare observation. Crack densities in the center 0-deg plys were relatively constant at various positions on the tank. However, the densities on 90-deg plys varied significantly. In some sections the inner 90-deg ply had a high density while the outer ply had a low density. In some sections, the trend was reversed. This suggests there may have been bending moments on the inner skin.

Tensile specimens were cut from the inner skin of the tank. Specimens were cut in the 0-, 45-, and 90-deg orientations. These specimens were tensile tested to incrementally higher loads. The sample was examined for microcracks between each loading cycle. These tests were performed at both 72 °F and –320 °F. As with the CBAT tests, the specimens were examined for microcracks after each load increment.

3. TEST RESULTS AND ANALYSIS

3.1 Mathematical Model of Microcracking

Two methods of modeling microcrack density in the two laminates were attempted. One method uses variational mechanics in conjunction with energy release rate failure.[2,3] A shear lag model in conjunction with energy release rate was also attempted. Garrett and Bailey,[4] and Lee and Daniel[5] have performed much work in the area of shear lag analysis on composite laminates. The shear lag/energy method of modeling in this report is based on the work performed by Laws and Dvorak[6] and McManus and Maddocks.[7,8]

Both methods result in a hyperbolic trigonometric function for crack density versus applied stress. Thus, the initial slope of the curve is infinite rather than small as observed in experimental data. The curves begin to match the experimental data as crack densities increase. So, both methods are more accurate for modeling progressive microcracking rather than the onset of microcracking.

The shear lag/energy model seemed to fit the experimental data better than the variational mechanics/energy model. Therefore, only that method will be discussed in this Technical Memorandum. To simplify modeling of the $(45F/\pm6T/90F_2/\pm6T)_s$ CBAT laminate, the ±6T plys were assumed to have the same transverse elastic properties as 0-deg plys. Based on the Classical Lamination Theory (CLT), there is little error in this assumption. However, this assumption and the orientation of the microcracks may explain why a higher critical strain energy release rate (G_{1c}) was observed in the CBAT laminate than the X–33 laminate.

If the transverse ply of interest is assumed to have a thickness of $2d$, the remainder of the composite is $2b$ (fig. 1). Stress is transferred to the transverse ply by shear between two cracks. At large crack spacing ($2h$), the stress within the transverse ply approaches that of an uncracked laminate. At high crack densities, the stress transfer is less effective.

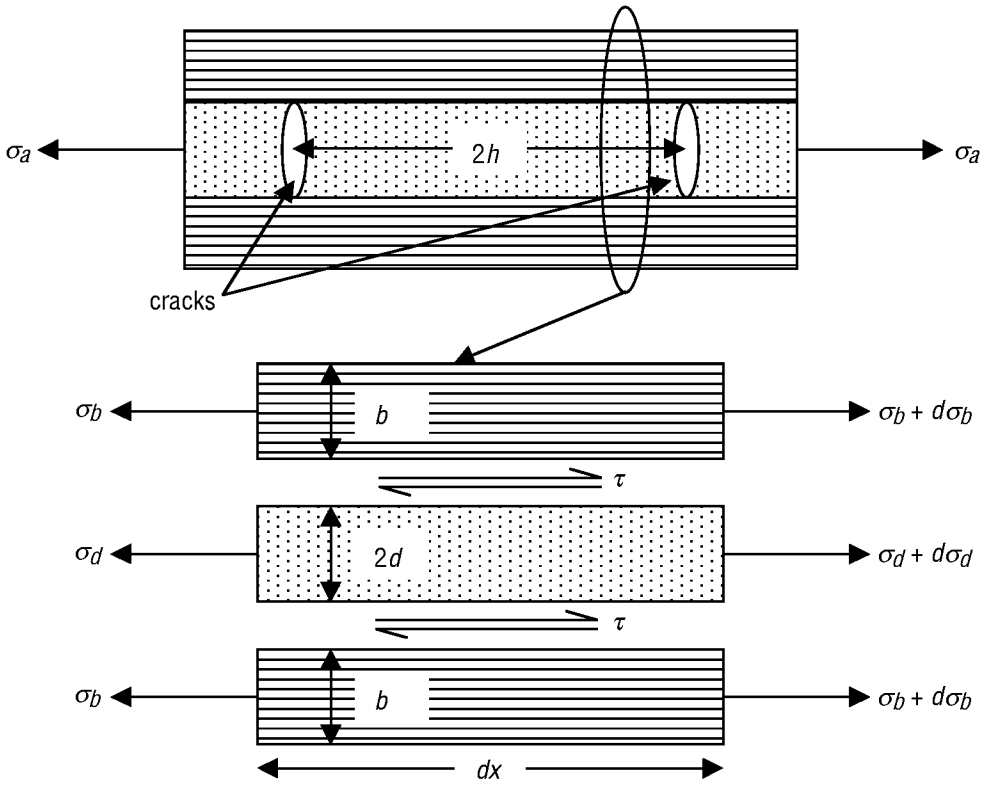

Figure 1. Shear lag model.

The shear lag analysis follows. Balancing forces in the laminate in figure 1 yields:

$$\tau = -b\frac{d\sigma_b}{dx} = d\frac{d\sigma_d}{dx} = H(u-v) \ , \tag{1}$$

where H is a constant and u and v are displacements in the b and d layers of the laminate. Various authors have presented differing values for the H constant. Garrett and Bailey suggest

$$H = \frac{G_{23}}{bd} \ , \tag{2}$$

while

$$H = \frac{3G_{12}G_{23}}{b\left(bG_{23} + dG_{12}\right)} \tag{3}$$

is suggested by Lee and Daniel. In either case the constant is proportional to the shear modulus of the transverse ply. Taking the second derivative of stress with respect to x gives:

$$\frac{d^2\sigma_d}{dx^2} = \frac{H}{d}\left(\frac{du}{dx} - \frac{dv}{dx}\right) \ , \tag{4}$$

where

$$\frac{du}{dx} = \varepsilon_b = \frac{\sigma_b}{E_b} + \alpha_b \Delta T \tag{5}$$

and

$$\frac{dv}{dx} = \varepsilon_d = \frac{\sigma_d}{E_d} + \alpha_d \Delta T \quad . \tag{6}$$

This results in the second order differential equation:

$$\frac{d^2\sigma_d}{dx^2} - \Phi^2 \sigma_d + F(\sigma) = 0 \tag{7}$$

where

$$\Phi^2 = \frac{HE_c(b+d)}{E_b E_d bd} \tag{8}$$

and

$$F(\sigma) = \frac{E_d}{E_o}\sigma_a - E_d(\alpha_d - \alpha_o)\Delta T. \tag{9}$$

$F(\sigma)$ is the sum of the mechanically induced stress and residual thermal stress on the transverse ply. The term could also incorporate other stresses such as those induced by moisture gain. The general solution[8] to the above differential equation is

$$\sigma_d = C_1 e^{\Phi x} + C_2 e^{-\Phi x} + \frac{F(\sigma)}{\Phi^2} \quad . \tag{10}$$

Solving for constants at the boundary conditions $\sigma_d = 0$ at $x = \pm h$ and simplifying the exponential terms by converting to hyperbolic terms results in the solution for tensile stress in the transverse ply,

$$\sigma_d = F(\sigma)\left(1 - \frac{\cosh(\Phi x)}{\cosh(\Phi h)}\right) \quad . \tag{11}$$

The shear stress at the interface of the transverse ply and the rest of the laminate (*b*-*d* interface) may also be determined by differentiating the stress,

$$\tau = d\frac{d\sigma_d}{dx} = d\Phi F(\sigma)\left(-\frac{\sinh(\Phi x)}{\cosh(\Phi h)}\right) \quad . \tag{12}$$

Based on the above equations, the stress distribution within the transverse ply can be plotted as a function of distance between two microcracks. The tensile stress within the transverse ply approaches the stress of the uncracked ply for large crack spacing. As the crack spacing decreases, the transverse ply carries less tensile load (fig. 2). However, the shear stress is still present. Thus, diagonal cracks begin to appear due to the shear stress at higher crack densities. These diagonal cracks are followed by delamination.

The strain energy can be used to predict the formation of microcracks. The Griffith energy theory states

$$\Delta G = \frac{dW}{dA} - \frac{dU}{dA} \quad , \tag{13}$$

where W is work, U is strain energy, and A is microcrack surface area. The change in work is the difference between work applied to the two cracked segments h after failure and the uncracked segment $2h$ prior to fracture. The strain energy is determined in the same manor. The strain energy release rate can be calculated as

$$\Delta G = \frac{\Phi d}{H} F(\sigma)^2 \left[2\tanh\left(\frac{\Phi h}{2}\right) - \tanh(\Phi h) \right] . \tag{14}$$

Theoretically, cracking initiates when $\Delta G > G_{1c}$, where G_{1c} is the critical strain energy release rate. However, due to defects and statistical variations in the properties of the composite, cracking will initiate at lower stresses than predicted. Thus, the first microcracks observed occur at strain energy release rates lower than G_{1c}. As the strain energy approaches G_{1c}, the microcrack density will rise rapidly. At higher microcrack densities, the transverse ply loses its ability to carry much tensile stress. Thus, the rate of increase in microcracks per applied stress begins to diminish.

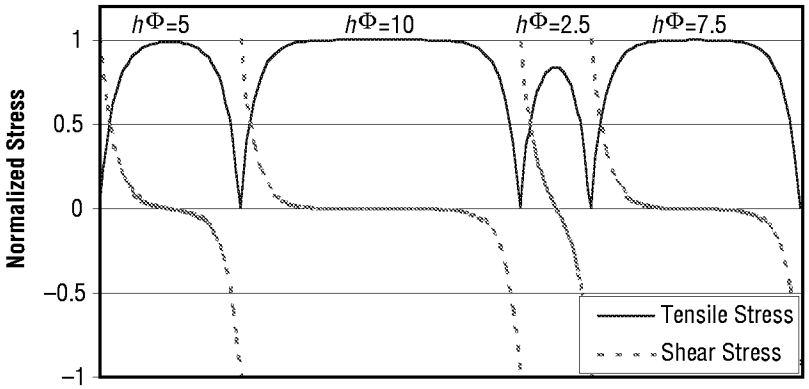

Figure 2. Stresses within a cracked ply of a composite laminate with various crack lengths ($2h$).

3.2 Composite Conformal, Cryogenic, Common Bulkhead, Aerogel-Insulated Tank

The microcracks in the CBAT laminate were not parallel to the fiber direction, +6 and –6 deg, as is typical of a cross-ply laminate. The cracks were perpendicular to the loading direction. Thus, the cracks periodically shift planes so the crack could penetrate both the +6 and the –6-deg plys (fig. 3). The crack density increases slowly with increasing load. The initial cracks may be defect related as in figure 4. As the load is further increased, the slope of the crack density versus applied stress increases dramatically. Eventually, as failure load is approached, the slope begins to decrease. This decrease in slope is because the transverse ply carries less load and other failure modes are beginning to occur. Figures 5 and 6 illustrate the trend in crack density versus applied load for the CBAT laminate.

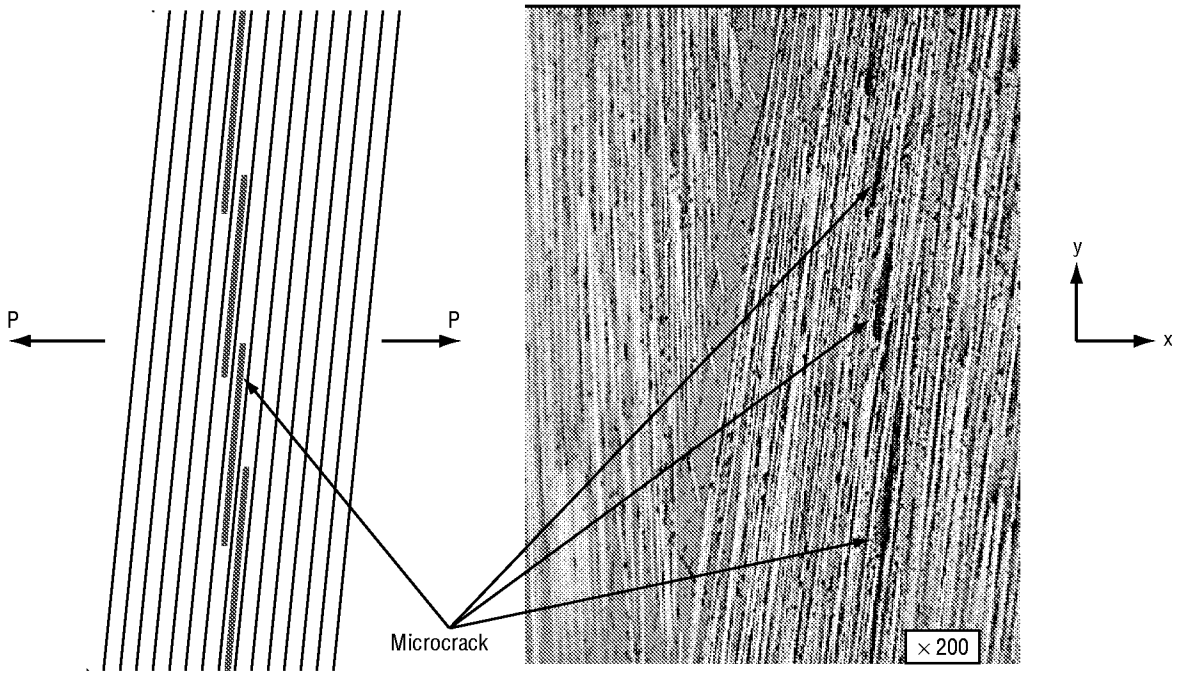

Figure 3. Crack in CBAT laminate (x–y plane).

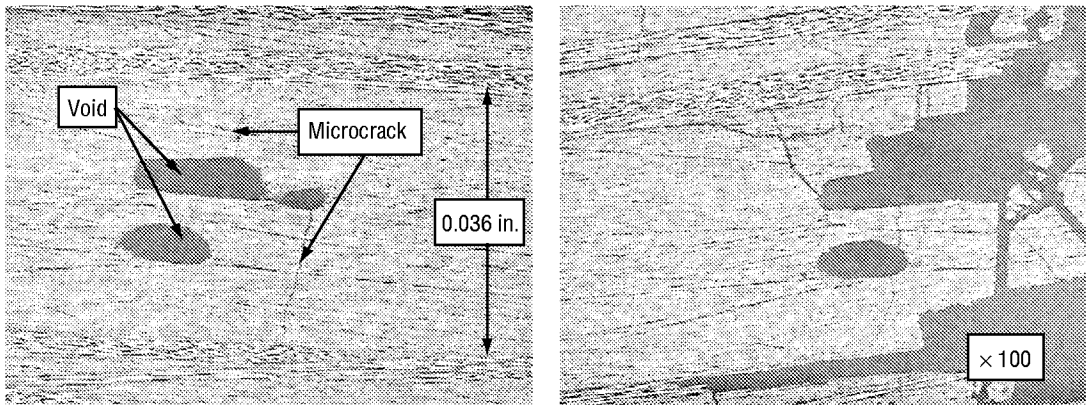

Figure 4. (a) First microcrack occurs on void and (b) failure occurs on the same void.

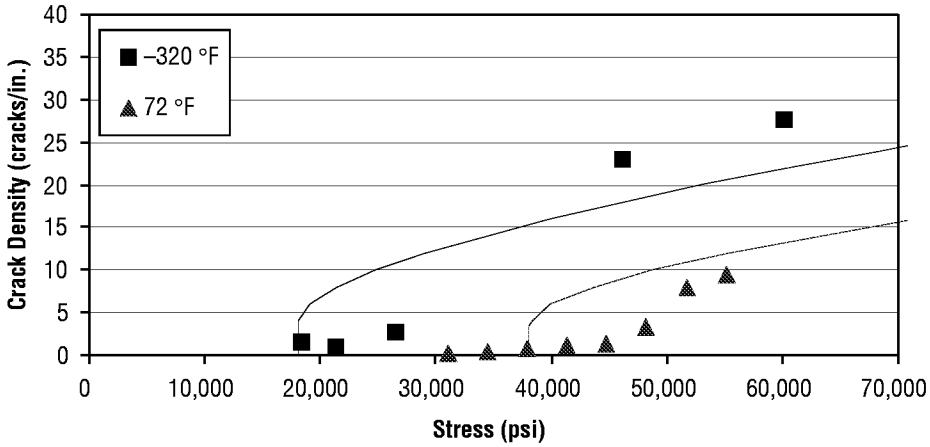

Figure 5. Crack density in $(+6/-6)_s$ ply of CBAT laminate versus applied tensile load.

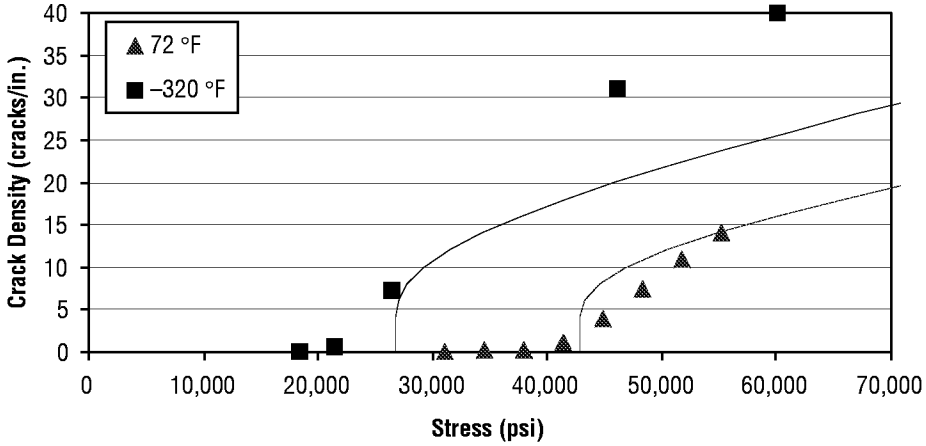

Figure 6. Crack density in (+6/–6) ply of CBAT laminate versus applied tensile load.

3.3 X–33 Liquid Hydrogen Tank

As with the CBAT laminate, a curve of microcrack density versus applied stress was produced. Again, microcrack initiation was gradual. The density then increased rapidly with increasing stress followed by a tapering of the slope prior to specimen failure.

The crack density versus applied load was calculated from equation (15). This was performed for both longitudinal and hoop orientations at 72, –320, and –423 °F. The G_{Ic} for 72 °F was chosen to fit the experimental data. From fracture mechanics,

$$G_{1c} = \frac{Q\sigma^2 h}{E} \tag{15}$$

where Q is a geometry factor. If all other parameters are constant, strain energy release rate (G) is inversely proportional to modulus (E). Thus, as the modulus increases due to cooling, the strain energy release rate decreases. The values used for G_{1c} were 1.3, 0.9, and 0.8 in.-lb/in.^{2} for 72, –320, and –451°F, respectively. These values are an order of magnitude lower than those reported by Nairn[2] and one-half those reported by Fiberite.[10] These lower values warrant further examination. Figures 7 and 8 illustrate the trend in crack density versus applied load for X–33 laminate.

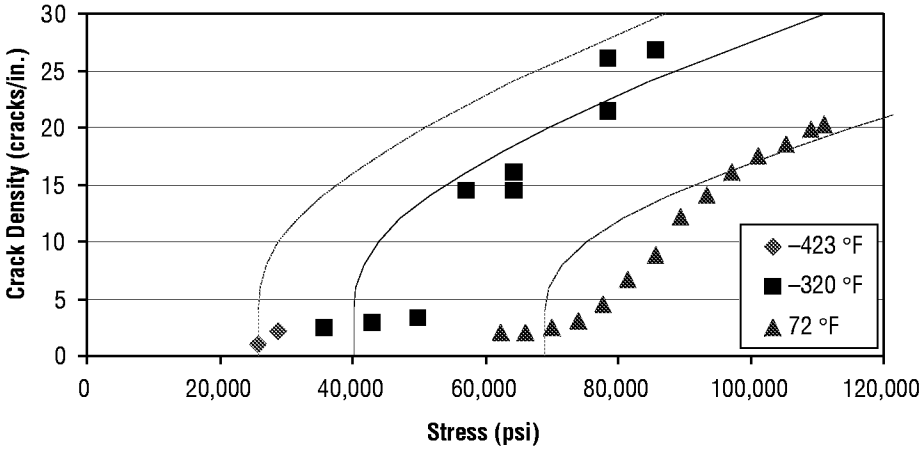

Figure 7. Crack density in hoop ply of X–33 laminate versus applied tensile load.

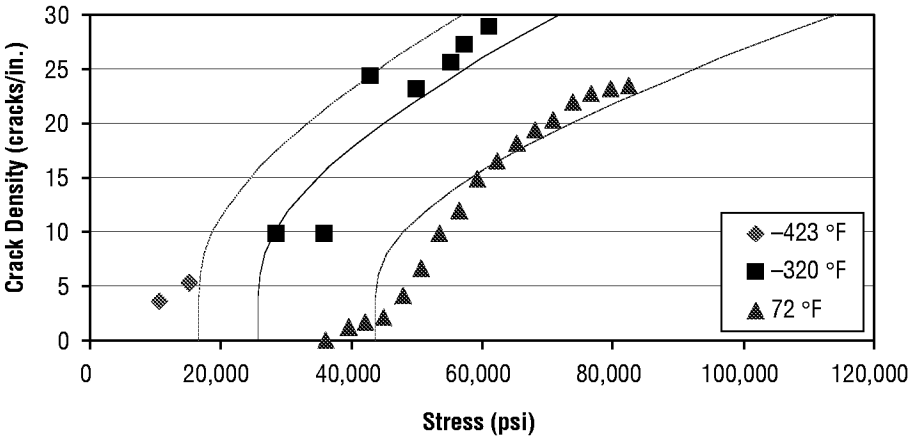

Figure 8. Crack density in longitudinal ply of X–33 laminate versus applied tensile load.

4. CONCLUSIONS

The shear lag/energy analysis modeled the crack density versus applied load quite well for the X–33 tank inner skin. The method was less successful at modeling the CBAT laminate. The CBAT laminate exhibited a higher crack density than predicted by the model. The model could more accurately predict microcrack density by adjusting the constant (*H*).

The model will not predict crack initiation since the first cracks that appear are due to defects and local variations in properties. A statistical approach should be used to model the initial cracking.

The modeling of crack density is highly dependent upon accurate elastic and thermoelastic properties over the temperature ranges evaluated. One problem with the current model is that it does not account for the temperature dependence of the CTE. The temperature dependence of the CTE makes the residual stresses within the laminate subject to error. Another problem is that the model is based upon uniaxial stress. A cryogenic tank, such as the X–33 tank, is subject to biaxial stress conditions. A laminate that is tensile tested to the same hoop or longitudinal stress conditions of the tank will be subject to different (generally higher) strains than the tank. Additional work is needed to further characterize the IM7/977–2 at LH_2 temperatures.

REFERENCES

1. Goetz, R.C.; and Ryan, R.S., Co-Chairs; and Whitaker, A.F., Vice-Chair: "Final Report of the X–33 Liquid Hydrogen Tank Test Investigation Team," Marshall Space Flight Center, AL, May 2000.

2. Nairn, J.A.; and Liu, S.: "The Formation and Propagation of Matrix Microcracks in Cross-Ply Laminates During Static Loading," *Journal of Reinforced Plastics and Composites*, Vol. 2, pp. 158–177, February 1992.

3. Nairn, J.A.: *Polymer Matrix Composites*, Talreja, R.; and Manson, J. A. (eds.): Chapter 13, "Matrix Microcracking in Composites," 2000.

4. Garrett, K.W.; and Bailey, J.E.: "Multiple Transverse Fracture in 90-Degree Cross-Ply Laminates of a Glass Fibre-Reinforced Polyester," *Journal of Materials Science*, Vol. 12, 1977, pp. 157–168.

5. Lee, J. W.; and Daniel, I.M.: "Progressive Transverse Cracking of Crossply Laminates," *Journal of Composite Materials*, Vol. 24, pp. 1225–1243, November 1990.

6. Laws, N.; and Dvorak, G.J.: "Progressive Transverse Cracking in Composite Laminates," *Journal of Composite Materials*, Vol. 22, pp. 900–918, October 1988.

7. McManus, H.L.; and Maddocks, J.R.: "On Microcracking in Composite Laminates Under Thermal and Mechanical Loading," *Polymers and Polymer Composites*, Vol. 4, No. 5, pp. 305–313, 1996.

8. Maddocks, J.R.; and McManus, H.L.: "Prediction of Microcracking in Composite Laminates Under Thermomechanical Loading," *NASA—CR–199800*, January 1995.

9. *CRC Standard Mathematical Tables*, CRC Press, Inc., 1984.

10. Fiberite Data Sheet, 977–2 toughened epoxy resin, 1995.

REPORT DOCUMENTATION PAGE

Form Approved
OMB No. 0704-0188

1. AGENCY USE ONLY *(Leave Blank)*	2. REPORT DATE	3. REPORT TYPE AND DATES COVERED
	August 2001	Technical Memorandum

4. TITLE AND SUBTITLE

Evaluation of Microcracking in Two Carbon-Fiber/Epoxy-Matrix Composite Cryogenic Tanks

5. FUNDING NUMBERS

6. AUTHORS

A.J. Hodge

7. PERFORMING ORGANIZATION NAMES(S) AND ADDRESS(ES)

George C. Marshall Space Flight Center
Marshall Space Flight Center, AL 35812

8. PERFORMING ORGANIZATION REPORT NUMBER

M–1024

9. SPONSORING/MONITORING AGENCY NAME(S) AND ADDRESS(ES)

National Aeronautics and Space Administration
Washington, DC 20546–0001

10. SPONSORING/MONITORING AGENCY REPORT NUMBER

NASA/TM—2001–211194

11. SUPPLEMENTARY NOTES

Prepared for Materials Processes and Manufacturing Department, Engineering Directorate

12a. DISTRIBUTION/AVAILABILITY STATEMENT

Unclassified-Unlimited
Subject Category 24
Nonstandard Distribution

12b. DISTRIBUTION CODE

13. ABSTRACT *(Maximum 200 words)*

Two graphite/epoxy cryogenic pressure vessels were evaluated for microcracking. The X–33 LH_2 tank lobe skins were extensively examined for microcracks. Specimens were removed from the inner skin of the X–33 tank for tensile testing. The data obtained from these tests were used to model expected microcrack density as a function of stress. Additionally, the laminate used in the Marshall Space Flight Center (MSFC) Composite Conformal, Cryogenic, Common Bulkhead, Aerogel-Insulated Tank (CBAT) was evaluated. Testing was performed in an attempt to predict potential microcracking during testing of the CBAT.

14. SUBJECT TERMS

composite, microcrack, cryogenic tank, tensile testing

15. NUMBER OF PAGES

20

16. PRICE CODE

17. SECURITY CLASSIFICATION OF REPORT	18. SECURITY CLASSIFICATION OF THIS PAGE	19. SECURITY CLASSIFICATION OF ABSTRACT	20. LIMITATION OF ABSTRACT
Unclassified	Unclassified	Unclassified	Unlimited